PM flux-reversal machine for wind energy application

Manne Bharathi[1], I. S. N. V. R. Prasanth[2], Tellapati Anuradha Devi[3], Malligunta Kiran Kumar[4], D. Ravi Kumar[5], Ch. Rami Reddy[6,7]

[1]Department of Electrical and Electronics Engineering, Vignan's Foundation for Science, Technology and Research, Guntur, India
[2]Department of Mechanical Engineering, Malla Reddy Engineering College, Secunderabad, India
[3]Department of Electrical and Electronics Engineering, Vardhaman College of Engineering, Shamshabad, India
[4]Department of Electrical and Electronics Engineering, Koneru Lakshmaiah Education Foundation, Guntur, India
[5]Department of Electrical and Electronics Engineering, VNR Vignana Jyothi Institute of Engineering and Technology, Hyderabad, India
[6]Department of Electrical and Electronics Engineering, Joginpally B.R. Engineering College, Hyderabad, India
[7]Applied Science Research Center, Applied Science Private University, Amman, Jordan

Article Info

ABSTRACT

Currently, attempts are being made to harness wind energy by means of non-conventional electrical machines such as flux reversal machines (FRM). The main advantage of the FRM, when compared with existing synchronous generators (SG), is that all the active parts like PMs and armature windings are mounted on the stator part, whereas leaving the rotor has simple and robust. In this study, the three-phase 6/8-pole flux reversal generators (FRGs) are selected, sized, designed, and analyzed using finite element analysis (FEA). The working principle, choice of stator and rotor poles, and machine design dimensions evaluation (analytical sizing procedure), as well as relevant performance details are discussed in this paper. This study is used to analyze, a popular 6/8 pole, 0.8 kW, 50 Hz, and examine the suitability for the wind energy applications in terms of torque and power density, torque ripple, power factor, and cogging torque under 2D finite element analysis (FEA). The analysis provides an update on the current state-of-the-art and as well as future thrust areas of research necessary to bridge the gap on what is still desired for the practical application of FRMs for wind energy.

Corresponding Author:

Malligunta Kiran Kumar
Department of Electrical and Electronics Engineering, Koneru Lakshmaiah Education Foundation
Guntur, Andhra Pradesh, India
Email: kiran.malligunta@gmail.com

1. INTRODUCTION

The usage of permanent magnet (PM) type electrical machines significantly growing day by day because the advantages of high-power and torque density, and efficiency, especially for variable speed drives for wind power generation [1]. The need for increased use of wind power generation is well established, because of its accessibility throughout the day and possibility for large megawatts power generation [2]. In 2020, the wind energy generation is a rapidly growing, economically practical, and highly efficient mode of electric power generation, with a global cumulative capacity of installed wind energy is 743 GW. The new installed global wind energy capacity was 93 GW as of 2020 as shown in Figure 1, which was a 53% increase when compared to 2019 [3]. The International Energy Agency (IEA) annual growth of global wind energy installation capacity forecast is a minimum of 14%. This encourages the researcher's interest in designing and manufacturing wind generators for various power levels. Wind energy generators acquire various types of AC generators, such as induction generators, permanent magnet synchronous generators (PMSG), and non-conventional stator PM generators. The PMSG with PMs on the rotor are attractive for large megawatts of

wind energy generation applications because of their high energy yield compared to other conventional electrical generators [4]. However, rotor PM structures are not good at high powers and speeds because they lead to mechanical instability problems. To this end, stator-mounted PMs have been developed and commercialized successfully for various applications.

Generally, PM machines are classified based on the position of the PMs, rotor PMs, and stator PMs. The existing PMSG are not suitable for low-speed and variable-speed applications [5], because it require heavy mechanical gears to connect with the wind turbines. Therefore, non-conventional stator-excited PM machines (SEPMMs) have been proposed for various applications [6]. SEPMMs are most suitable in commercial applications compared to the existing electrical machines due to their many advantages. Compared to the rotor-excited PM machine, SEPM machines are preferable because rotating PMs may cause irreversible demagnetization problems, and limit the power density and mechanical instability [7], [8]. There are two types of SEPMMs: flux reversal machines (FRM) and flux switching machine (FSM). The first one is a double salient SEPMM called a flux switch alternator. When Rauch and Johnson [8] first introduced it in 1955, the rotor volume usage was found to be poor, producing stator vibrations and difficulty in stator assembly. To enhance the torque density and to help simplify the manufacturing process, Deodhar *et al*. [9] invented a single-phase FRM to replace the standard claw pole alternator for automobile applications in 1997. Wang *et al*. [10] introduced the three-phase FRM in 2000. The machine design was optimized from one phase to three-phase to enhance high PM flux-linkage at the armature winding, good electromagnetic performances, and less cogging torque. Although the FRM was not the first double salient PM electrical machine, it has bipolar phase, magnetic motive force (MMF), and flux variation with regard to the rotor rotation. It also seems that FRM, inherently have low self and mutual inductance with rotor displacement and so, it has a low electrical time constant. All these features, incorporated with a simple structure of FRM, make it attractive for low-cost variable speed generator design [11].

Further, to increase the power density of FRM, full-pitched winding is introduced rather than concentrated winding, and it is also compared with PMSG by introducing the "fictitious electrical gear" concept [12]. It is claimed that full-pitched flux reversal generator (FRG) stator winding is twice as efficient as concentrated FRG winding, but this would result in increases in self-inductance is 2.5 to 3 times depending on the saturation of the machine, which leads to poor voltage regulation. It is improved with series capacitive compensation and compared power density in terms of PMSG, the full-pitched stator winding of FRG is 13.75% higher, making this structure a suitable competitive one for low-speed drives [12], [13]. In [14], [15], comparisons are made between 6/14 rare earth FRG and 28-pole fractional slot PMSG under similar physical dimensions, rated speed, and electrical and magnetic loading. The authors concluded that the power density of 6/14 FRG is 1.5 times that of the 28-pole fractional slot PMSG and that the power factor and voltage regulation of PMSG are slightly better than those of FRM. Further, it is claimed that the constant power speed range of FRM is better than PMSG, making it the most suitable for low-speed, low-power applications.

Figure 1. The global installation wind energy market capacity

In More *et al*. [16], an outer rotor 6/14 FRM structure with rare earth PMs for rooftop wind turbine generators was introduced, and when compared to a 6/14 inner rotor structure with the same outer dimensions, it was stated that the outer rotor FRM has 1.25 times higher power density than the inner rotor and improved the machine's performance for direct drives. In [17]-[20], a 10 kW, 50 rpm, 12/64 FRM structure with rare earth (Nd-Fe-B) was developed and optimized in terms of mass-to-torque ratio through the finite element method for low-speed direct drives. In [20], [22], FRM with a 48/46 structure with rare earth (RE) PMs has been developed for gearless direct drive wind power generation applications and compared with PMSG, claimed that usage of rare earth PMs is 5 times less than PMSG with magnets on the rotor. Active material cost is also 2.3 times less, because the toothed FRM rotor structure is simple and reliable, only made up of laminated steel, and overall machine manufacturing is also 1.3 times less than PMSG. Furthermore, it stated that FRM maintains high efficiency with a wide speed range and ripple torque is low as with rotor PMs generator [23]. The recent studies of FRM designs and abound for various applications clearly show that RE-excited FRMs are emerging. Such studies appear that these FRM generators are suitable replacements for RE rotor excited brushless type machines [24]. Most of the existing literature has focused on the analysis of small power scale (above 1 kW) ratings which are employed for the high-speed (HS) or low-speed (LS) drivetrains, to indicate a need to investigate the performance of RE FRMs scaled to the below 1 kW range for medium speed (MS) roof-top wind energy applications [25]. The MS speed drive trains are popular and good correlation between the size and cost of both generator and mechanical drivetrain systems.

The main contribution of this study is used to explore the potentials of RE FRMs is in the application of roof-top wind energy generator modeling and employed to medium-speed wind generator drives at micro power scale. The aim of this paper is used to explore the potentials are RE PMs of a 6/8 pole, FRMs topology for MS wind power generation applications at micro power-scale. In this study, a 3 phase, 6/8 pole FRM of PMs generator is designed with characterization for 0.8 kW power scale is investigated. Thus, an overview of the FRM technology including the operating principle, desirable stator-slot and rotor pole combinations is discussed with flux distribution under 2D finite element analysis (FEA) in section 2. Therefore, in section 3, the design formulation of the FRM, a pseudo-optimal parametric variation procedure to evaluate the design dimensions is investigated at 2D FEA for MS drivetrains. Further, the power-generating performances of the FRMs are considered in this study in terms of terminal voltage, voltage regulation, torque power density, and efficiency at rated load conditions are explained in section 4. The section 5 presents the concluding remarks.

2.   BASIC PRICIPLE OF FRM

The FRMs operating principle is explained with the help of a popular 3-phase, 6/8 pole FRM structure. Two coils in a series make a phase. Typical 2D and 3D cross-sections of this FRM are illustrated in Figure 2. With respect to Faraday's law of electromagnetic induction, the rotation of the rotor changes the permeance in airgap, which leads to a change in the flux linkage ψ_m in stator coils by field source at a given electrical speed (ω_e). A bipolar induced electromotive force (EMF) appears on the stator terminals e_o which is given as (1).

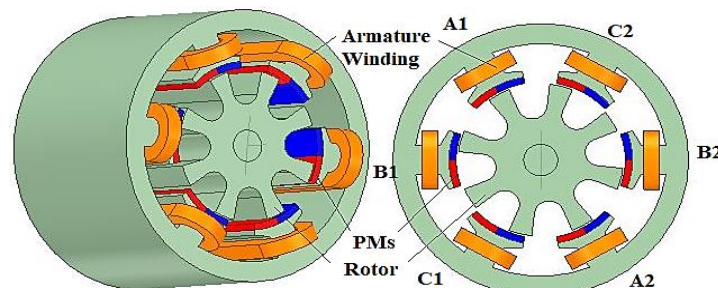$$e_o = -\omega_e \frac{d\psi_m}{d\theta} \qquad (1)$$

Figure 2. A structural view of 2D and 3D view of a 6/8 pole FRM

When a prime mover spins the rotor, in the case of a generator, the FRM principle can be demonstrated based on 2D static FEA line flux density distribution plots, as depicted in Figure 3. In Figure 3(a), a rotor pole is between two PMs at the stator top part and the PMs in the stator bottom pole. This position is called an

equilibrium position, in which the rotor poles and stator pole PMs are not aligned; the flux produced by the PMs moves wholly in each stator teeth, with there is no flux in the stator core [11].

When the rotor is driven by 11.2° in a counter-clockwise direction (CCWD), the rotor poles are aligned with the PMs, and the flux passes through coils, stator core, top PMs, and bottom PMs. In this position, as depicted in Figure 3(b), the flux is maximum. In Figure 3(c), the rotor is further moved from the initial equilibrium position by 22.5°, there is no flux in the stator yoke and no flux linking with the armature winding coils. Further, rotor movement of 11.25° in the clockwise direction (CWD) results in the position illustrated in Figure 3(d). In this position, the flux is again maximum. However, this position is opposite to that of the first alignment in Figure 3(b). From all these, it can be seen that FRM has a bipolar flux variation and MMF considering the rotor displacement and it covers all four quadrants. At the positions in Figures 3(a) and 3(c), there are zero-flux linkages, while at those in Figures 3(b) and 3(d), the energy transformation occurs, and the flux reversal concept is established.

(a)   (b)

(c)   (d)
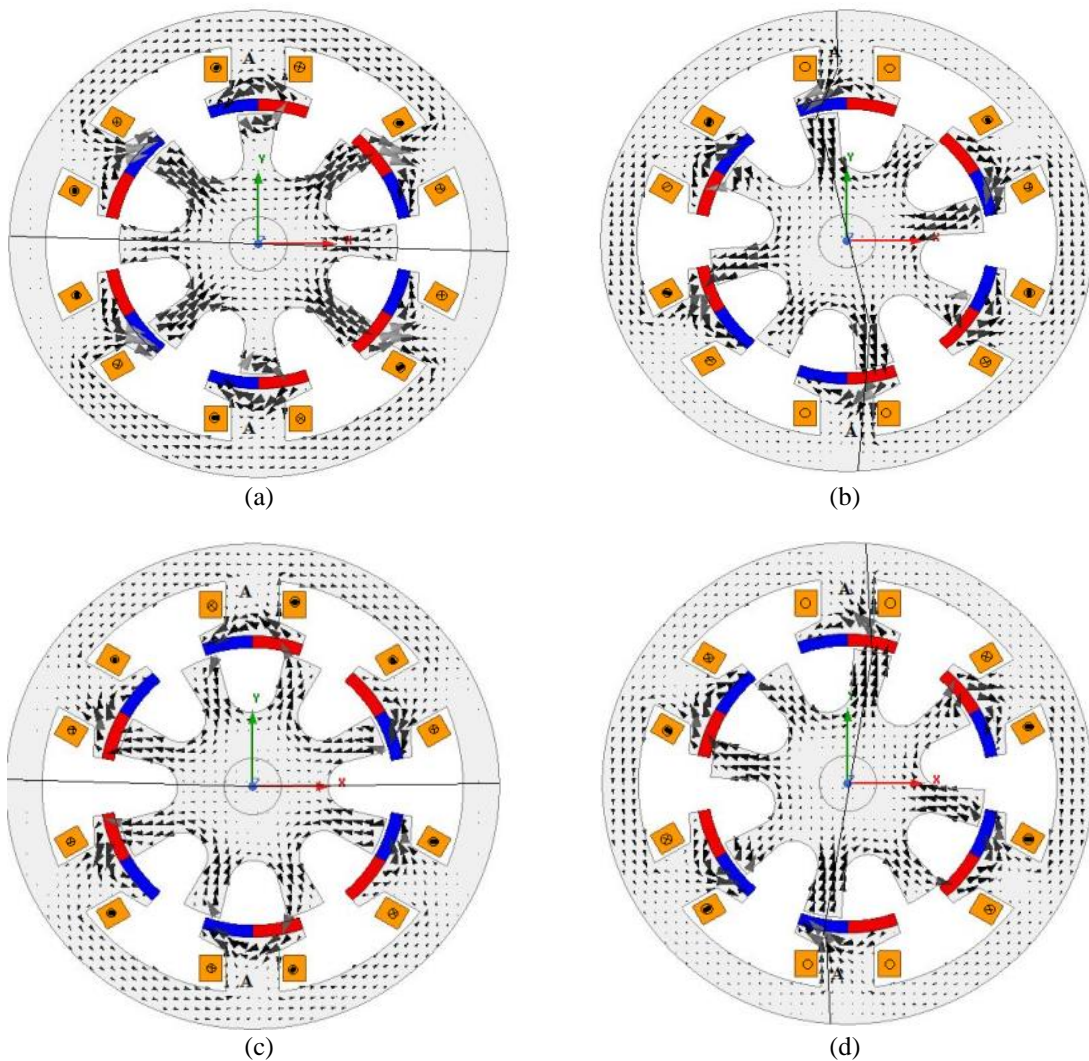
Figure 3. The working principal of 6/8 of 6/8 stator-slot/rotor-pole FRM (a) a rotor displacement at 0°, (b) a rotor displacement at 11.25° CCWD, (c) rotor displacement at 22.5° CCWD, and (d) rotor displacement at 11.25° CWD

3.   DESIGN FORMULATION OF FRM

A popular, 3-phase, 6/8 pole FRM structure can be chosen, these combinations can achieve symmetrical phase EMF with higher torque and power density [13]. The lower number of rotor pole (N_r) and stator slot (N_s) count is recommended for the minimization of core losses and manufacturing difficulty,

although a lower number of poles leads to a minimization in the amplitude of EMF [13]. Based on all the limitations, a negotiation between and frequency (50 Hz) and high amplitude EMF, a 6/8 FRM topology is employed. Considering the machine rotor speed (n) and open circuit EMF frequency (f_e) as expressed by (2).

$$f_e = \frac{n * N_r}{60} \tag{2}$$

The preliminary design dimensions of a 6/8 pole FRM are evaluated, based on the rated power requirement as micro-scale (0.8 kW) at @ 375 r/min. As a generator, the electromagnetic power P_{eb} at a desired efficiency of 0.95 and speed of 375 r/min is given by (3).

$$P_{eb} = \frac{rated\ power}{efficiency} \tag{3}$$

Then, the specific electrical and magnetic loading are assumed to evaluate the tangential force density f_t. The general output sizing procedure to model the machine is expressed as (4) [13].

$$D_r = \sqrt[3]{\frac{2P_b}{\pi f_t \lambda \omega_r J \eta}} \tag{4}$$

Where ω_r is rotor speed (rad/sec), η is machine efficiency, λ is machine laminated stack to rotor diameter, and the designed FRM structure is needed to operate the machine to meet with wind turbine power rating for a MS drivetrain. The key evaluated parameters and dimensional specifications of the FRM machine for MS drives are presented in Table 1.

Table 1. Key design dimensions and parameters of the FRM

Parameter/dimension	RE-FRG
Rotor pole span angle ($\alpha=\beta$), deg	22.5
Number turns per coil (N_t)	176
Stack length (l_{stk}), mm	200
Stator outer diameter (D_{out}), mm	129
Outer rotor diameter (D_r), mm	72
Stator pole width (w_{ts}), mm	21
Rotor pole height (h_{pr}), mm	17
Current density(J) (A/mm^2)	5
Stator back iron thickness (B_{cs}), mm	11
Slot opening width (l_{wi}), mm	29
Shaft diameter (D_{sh}), mm	46
Rated speed, (r/min)	375
Magnet thickness (h_{pm}), mm	3
Rated frequency (Hz)	50
Fill factor (k_{fill})	0.4

Thereafter, tangential force densities from equivalent electric and magnetic loading of the machines can be selected based on the literature studies [14], [15] of FRMs. Further, based on the sizing expression in (4), the rotor diameter and stack length can be evaluated. After choosing the appropriate residual flux density and coercive force parameters etc. for specific PMs, the airgap flux density can be evaluated. A detailed structural parameter of rotor and stator can then be derived. FEA is then used to validate the generator design specifications. There should be a check to verify that the machine geometry parameters are practical. If not, the initial values should be reset. FEA verifications at various operation conditions are then conducted, its process is flow charted and presented in Figure 4. With 2D FEA, the power-generating performances such as flux linkages, EMF, CT and ripple torque, power and torque density, good smooth average torque, etc., are investigated. If desired performances are not achieved, the design flow can be iterated with adjustments made to the design parameters. This can be observed in Table 1, that the 2D FEA and analytical results have good correlations. Hence, a conclusion can be drawn that the proposed analytical design methodology is effective and applicable.

The 2D geometrical dimensional view of 3-phase FRM can be depicted in Figure 5. From the magnetostatic simulation, the open-circuit flux density of FRM is B=1.2 T for rare-earth (Nd-Fe-B) and the mesh plot can be depicted in Figure 6 from the 2D FEA. Relative permeability μ_r=1.09 and field intensity H_c= 900 kA/m is considered throughout the machine design. The other design constraints are assumed, that are filling factor and current density, can be chosen based on the cooling mechanism [14]-[17], 5 A/mm^2, and 0.4, respectively. From MS no-load a CT of the FRM is examined under 2D FEA and the peak-to-peak CT is 2.45 Nm as shown in Figure 7.
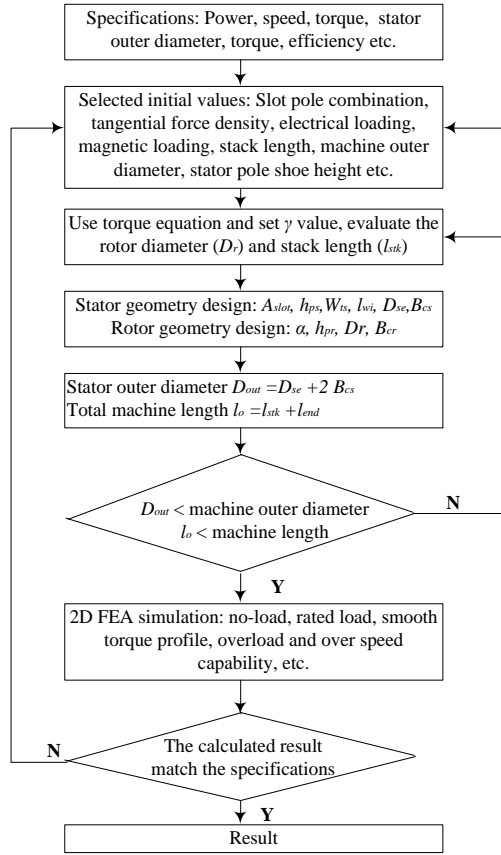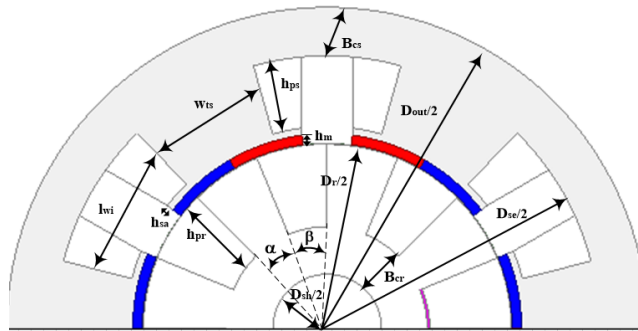
Figure 4. Design flow chart of FRM
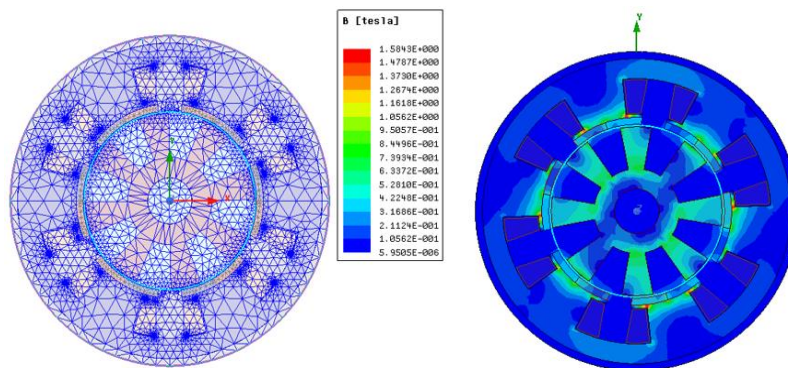

Figure 5. Geometrical view of the FRM

Figure 6. 2D FEA evaluation of mesh plot and flux density plot
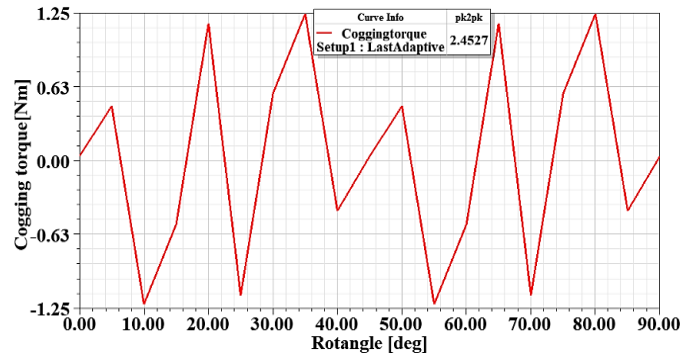
Figure 7. The cogging torque variation of FRM at magnetostatic condition

4. PERFORMANCE EVALUATION OF FRM

Many of the studies have developed different FRM topologies for wind turbine applications. Many of the studies regarding are high-speed or low-speed wind applications at low power levels only [18]-[21]. In this study is used to consider the MS drive train system for FRMs, as like of other drive trains, which are already examined for the brushless double salient structures [22]-[24]. In this study, a 6/8 pole, 375 r/min, micro power level, Nd-Fe-B excited FRM structure are studied and developed at 2D FEA, for MS wind energy generator applications. The power generating performance are analyzed, with respect to torque and power density, terminal voltage, efficiency, and power factor at the rated load conditions are analyzed.

4.1. Open circuit condition (no-load) analysis

This FRM structure is investigated under the no-load or open circuited condition, under 2D FEA. The open-circuited condition, the flux linkages, voltages, and CT are investigated. The phase flux linkages and voltages at no-load are presented in Figures 8 and 9. An interesting fact to note about the cogging torque that the transient analysis show that the CT is lower at magnetostatic than with transient no-load due to the presence of excitations or speed to the FRM, less locking is experienced between the rotor and PMs can be presented in Figure 10. The CT is a function of torque ripple at load condition, so, it required to minimize the PM excited machines for the safe operation [20]. By considering the optimal design dimensions the cogging torque and torque ripple are minimized compared with existing PM machines.

4.2. On-load analysis

The electromagnetic performances at load condition are analyzed and the rated load resistance of the generator can be evaluated under rated power and voltage of each phase, i.e., R_n is 25.3 Ω. In this section is used to examine the power generating performances of the FRM including terminal voltage against phase current, voltage regulation, torque ripple, efficiency, and power factor, as well as losses are analyzed by the 2D FEA.

In the actual run condition, the torque ripple of the FRM at rate load condition is depicted in Figure 11. In the load condition torque ripple is the function of the cogging torque, which leads to vibration and noise at load, and it creates negative impact on the machine performance. The torque ripple of FRM can be evaluated from the graph that peak-to-peak torque to avg torque under the load.
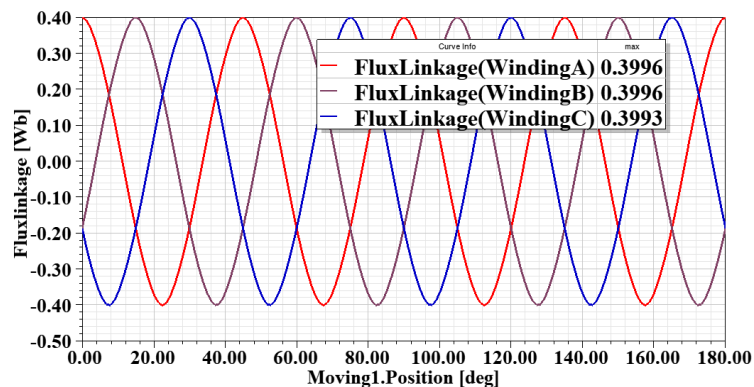

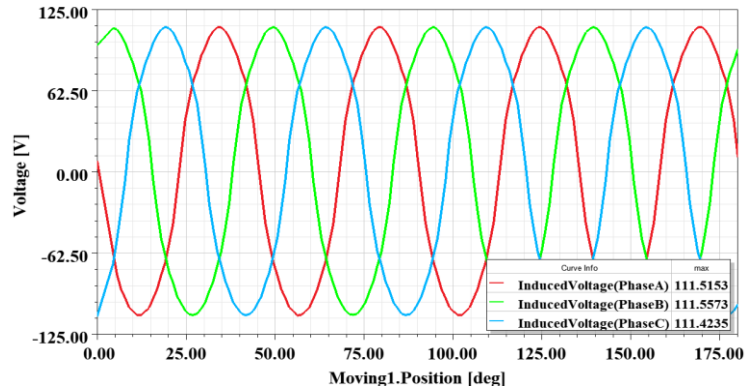Figure 8. The transient open-circuited flux linkage plot of FRM

Figure 9. The open circuited each phase voltage of FRM @ 375 r/min
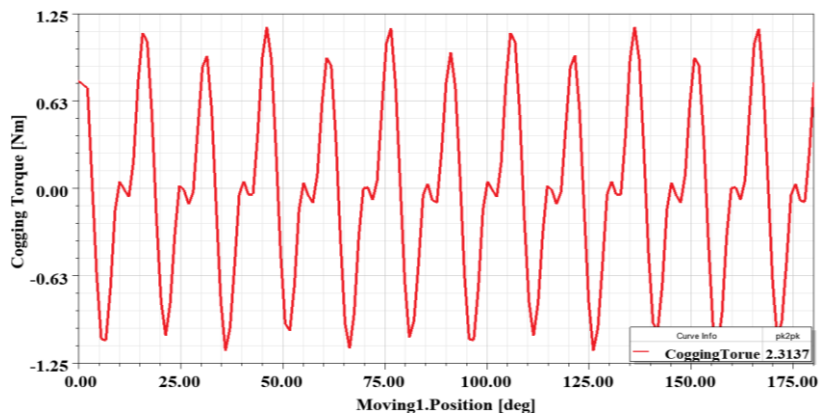

Figure 10. The cogging torque effect of FRM under no-load
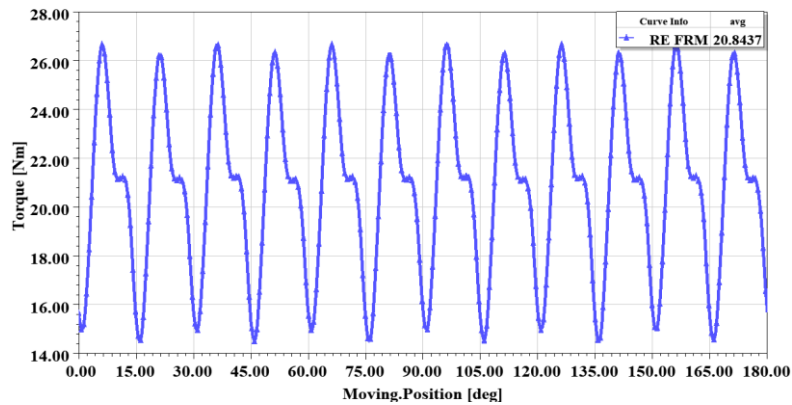

Figure 11. Torque ripple effect of the FRM

The output voltage (rms), current (rms), and power of the machine when operating at resistive load @ 375 r/min are analyzed through FEA to investigate the overload capabilities of the machines. The generating operating point performances including output voltage against load current, voltage regulation, power curve in terms of varying load current and machine speed, as well as loss and efficiency curves of the machine working is analyzed by FEA simulation. The transient load condition the output voltage against load current curve is plotted to examine the overload capability can be depicted in Figure 12. From Figure 12, observe that as load current increases the FRM exhibits good overload capability. The torque density of the RE machine is higher because it has higher remanence flux density and coercive forces. Further, the electromagnetic performances are of output power, torque density, efficiency, power factor is analyzed, and overall performances are summarized from 2D FEA and presented in Table 2.
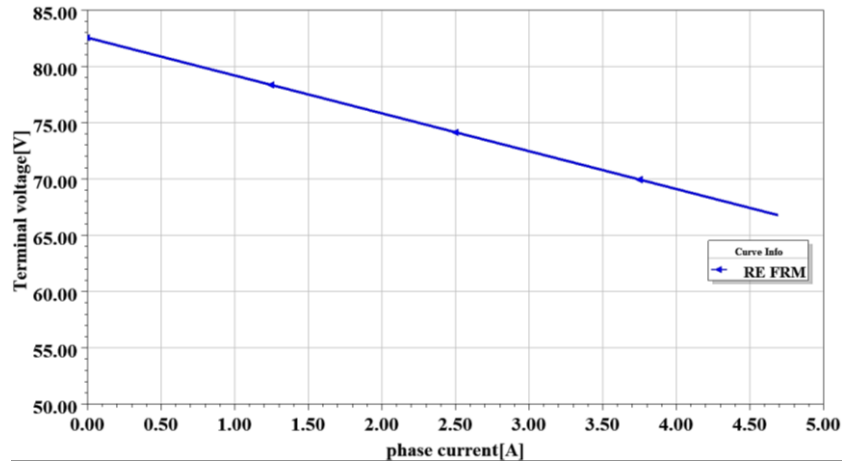
Figure 12. The output voltage vs the phase current @ 375 r/min

Table 2. 2D FEA predicted characteristics of the 3-phase, 6/8 pole FRM under the load condition

Parameter	FRM
Torque ripple under rated load, %	11.46
Output voltage [RMS] (V)	82
Rated output power (kW)	0.863
Voltage regulation (%)	12.75
Efficiency at rated load %	93
Torque density (kNm/m^3)	38.671
Total losses at rated load, W	47.49
Power factor	0.8

5. CONCLUSION

In this paper, the need for investigating the potential of PM excited FRMs for the medium speed wind energy applications at the micro scale has been studied. A 3- phase, 6/8 pole rare-earth FRM structure were modelled based on analytical design-sizing procedure (pseudo-optimal parametric variation), semi-optimized FRMs and simulated under 2D FEA, then considering some other design constraints for medium speed drives and implemented in the 2D FEA environment. The peak-to-peak cogging torque and torque ripple (%) are examined at transient no-load i.e., 2.31 Nm and 0.1146 respectively. The designed machine exhibits better overload capability when the load current is varied up to 1.5 times of the rated load. Further, the torque density and power factor are examined, i.e, 38.6 kNm/m^3 and 0.8 respectively. Based on the overall performance summary of the proposed machine exhibits good overload capability, torque density, efficiency and power factor, this structure is best suitable for medium speed wind turbine generator applications.

REFERENCES

[1] M. Chinchilla, S. Arnaltes, and J. C. Burgos, "Control of permanent-magnet generators applied to variable-speed wind-energy systems connected to the grid," *IEEE Transactions on Energy Conversion*, vol. 21, no. 1, pp. 130–135, 2006, doi: 10.1109/TEC.2005.853735.
[2] U. B. Akuru and M. J. Kamper, "Evaluation of flux switching PM machines for medium-speed wind generator drives," *2015 IEEE Energy Conversion Congress and Exposition (ECCE)*, 2015, pp. 1925–1931, doi: 10.1109/ECCE.2015.7309932.
[3] IEA, "Energy and climate change - World energy outlook special report," *International Energy Agency*, 2016, [Online]. Available: http://www.worldenergyoutlook.org/media/.
[4] GWEC, "Global wind energy report – Special Report," *Global Wind Energy Council*, 2021, [Online]. Available: https://gwec.net/global-wind-report-2021/.
[5] U. B. Akuru and M. J. Kamper, "Design and Investigation of Low-cost PM Flux Switching Machine for Geared Medium-speed Wind Energy Applications," *Electric Power Components and Systems*, vol. 46, no. 9, pp. 1082–1090, 2018, doi: 10.1080/15325008.2018.1485789.
[6] M. Cheng, W. Hua, J. Zhang, and W. Zhao, "Overview of stator-permanent magnet brushless machines," *IEEE Transactions on Industrial Electronics*, vol. 58, no. 11, pp. 5087–5101, 2011, doi: 10.1109/TIE.2011.2123853.
[7] D. K. Jang and J. H. Chang, "Performance comparison of PM synchronous and PM vernier machines based on equal output power per unit volume," *Journal of Electrical Engineering and Technology*, vol. 11, no. 1, pp. 150–156, 2016, doi: 10.5370/JEET.2016.11.1.150.
[8] S. E. Rauch and L. J. Johnson, "Design Principles of Flux-Switch Alternators [includes discussion]," *Transactions of the American Institute of Electrical Engineers. Part III: Power Apparatus and Systems*, vol. 74, no. 3, Jan. 1955, doi: 10.1109/AIEEPAS.1955.4499226.

[9]   R. P. Deodhar, S. Andemon, I. Boldea, and T. J. E. Miller, "The flux-reversal machine: a new brushless doubly-salient permanent-magnet machine," *IEEE Transactions on Industry Applications*, vol. 33, no. 4, pp. 925-934, Jul-Aug. 1997, doi: 10.1109/28.605734.

[10]   C. Wang, S. A. Nasar, and I. Boldea, "Vector Control of Three-Phase Flux Reversal Machine," *Electric Machines & Power Systems*, vol. 28, no. 2, pp. 153–166, Feb. 2000, doi: 10.1080/073135600268432.

[11]   C. X. Wang, I. Boldea, and S. A. Nasar, "Characterization of three phase flux reversal machine as an automotive generator," *IEEE Transactions on Energy Conversion*, vol. 16, no. 1, pp. 74–80, Mar. 2001, doi: 10.1109/60.911407.

[12]   D. S. More and B. G. Fernandes, "Analysis of flux-reversal machine based on fictitious electrical gear," *IEEE Transactions on Energy Conversion*, vol. 25, no. 4, pp. 940–947, 2010, doi: 10.1109/TEC.2010.2048330.

[13]   D. S. More, H. Kalluru, and B. G. Fernandes, "Comparative analysis of flux reversal machine and fractional slot concentrated winding PMSM," in *IECON Proceedings (Industrial Electronics Conference)*, 2008, pp. 1131–1136, doi: 10.1109/IECON.2008.4758113.

[14]   V. Dmitrievskii and V. Prakht, "Gearless generator with magnets on the stator for wind turbine," in *Journal of Physics: Conference Series*, 2018, vol. 1102, no. 1, doi: 10.1088/1742-6596/1102/1/012018.

[15]   L. Shao, W. Hua, M. Cheng, J. Soulard, Z. Wu, and Z. Q. Zhu, "Electromagnetic performance comparison between 12-phase switched flux and surface-mounted PM machines for direct-drive wind power generation," in *IEEE Transactions on Industry Applications*, vol. 56, no. 2, pp. 1408-1422, 2020, doi: 10.1109/TIA.2020.2964527.

[16]   D. S. More, H. Kalluru, and B. G. Fernandes, "Outer Rotor Flux Reversal Machine for Rooftop Wind Generator," in *2008 IEEE Industry Applications Society Annual Meeting*, Oct. 2008, pp. 1–6, doi: 10.1109/08IAS.2008.77.

[17]   G. Pellegrino and C. Gerada, "Modeling of flux reversal machines for direct drive applications," *Proceedings of the 2011 14th European Conference on Power Electronics and Applications*, 2011, pp. 1–10.

[18]   B. Vidhya and K. N. Srinivas, "Small Scale Wind Generation System: Part I – Experimental Verification Of Flux Reversal Generator Block," *International Journal of Applied Power Engineering (IJAPE)*, vol. 6, no. 1, p. 1, 2017, doi: 10.11591/ijape.v6.i1.pp1-12.

[19]   A. Mohammadi *et al.*, "Design Optimization of a Direct-Drive Wind Generator With a Reluctance Rotor and a Flux Intensifying Stator Using Different PM Types," *IEEE Transactions on Industry Applications*, vol. 60, no. 4, pp. 6113–6123, Jul. 2024, doi: 10.1109/TIA.2024.3396792.

[20]   S. Różowicz, Z. Goryca, and A. Różowicz, "Permanent Magnet Generator for a Gearless Backyard Wind Turbine," *Energies*, vol. 15, no. 10, 2022, doi: 10.3390/en15103826.

[21]   V. Prakht, V. Dmitrievskii, V. Kazakbaev, and M. N. Ibrahim, "Comparison between rare-earth and ferrite permanent magnet flux-switching generators for gearless wind turbines," *Energy Reports*, vol. 6, pp. 1365–1369, 2020, doi: 10.1016/j.egyr.2020.11.020.

[22]   M. Bharathi, U. B. Akuru, and M. K. Kumar, "Comparative Design and Performance Analysis of 10 kW Rare-Earth and Non-Rare Earth Flux Reversal Wind Generators," *Energies*, vol. 15, no. 2, 2022, doi: 10.3390/en15020636.

[23]   L. Szabo, "A survey on modular variable reluctance generators for small wind turbines," *IEEE Transactions on Industry Applications*, vol. 55, no. 3, pp. 2548–2557, 2019, doi: 10.1109/TIA.2019.2891730.

[24]   U. B. Akuru and M. J. Kamper, "Performance comparison of optimum wound-field and ferrite PM flux switching machines for wind energy applications," in *Proceedings - 2016 22nd International Conference on Electrical Machines, ICEM 2016*, 2016, pp. 2478–2485, doi: 10.1109/ICELMACH.2016.7732869.

[25]   M. Salehi, A. Ghaheri, A. Omidi, A. Darabi, M. H. Marzebali, and M. Manjrekar, "Transverse Flux Permanent Magnet Machines State of the Art and Design Procedure for Direct Drive Wind Turbines," in *2024 IEEE Transportation Electrification Conference and Expo (ITEC)*, Jun. 2024, pp. 1–6, doi: 10.1109/ITEC60657.2024.10599005.

BIOGRAPHIES OF AUTHORS

Manne Bharathi 🆔 ⑧ SC ↻ received B.Tech. degree in electrical and electronics engineering from PVP Siddhartha Institute of Technology, JNTU, Kakinda, India, in 2015, M.Tech. degree in power systems from Acharya Nagarjuna University,Guntur, India, in 2017 and received Ph.D. in electrical and electronics engineering at Koneru Lakshmaiah Education Foundation, Guntur, India in 2022. Her current research includes fuel cell modeling for distributed generation and grid connected applications and special electrical machines modeling and cogging torque minimization analysis especially for wind turbine generator applications. She can be contacted at email: bharathi.manne1994@gmail.com.

I. S. N. V. R. Prasanth 🆔 ⑧ SC ↻ was awarded a doctorate of philosophy in mechanical engineering (machining of composites) from Jawaharlal Nehru Technological University, Hyderabad, Post graduation in the specialization of industrial engineering and management from JNTUH and bachelor of engineering in mechanical engineering from JNTUH. He has 17 years of teaching experience in various reputed engineering colleges in Hyderabad. He is very much enthusiastic towards research activities. He has published 3 Free SCI, 6 Free Web of Science and 6 Free Scopus journal papers, 1 book chapter, 4 patents and around 30 other reputed publication papers. Reviewed ten articles in reputable international journals. Under his able guidance 32 projects have been completed in UG level, and 8 projects in PG level. One CRG project has been provisionally accepted in May-2023. He can be contacted at email: prasanth5109@gmail.com.

Tellapati Anuradha Devi working as assistant professor in the Department of Electrical and Electronics Engineering, Vardhaman College of Engineering has about 8 years of teaching experience. She received her B.Tech. degree in electrical and electronics engineering with distinction from V.R. Siddhardha Engineering College, Nagarjuna University, Vijayawada and M.Tech. degree in power electronics and drives with distinction from JNTU, Hyderabad and received Ph.D. degree in electrical and electronics engineering from Koneru Lakshmaiah Education Foundation, Guntur, Andhra Pradesh. Her research includes switched reluctance machines power electronics and electric vehicles. She can be contacted at email: anuradhadevi.eee@gmail.com.

Malligunta Kiran Kumar working as an associate professor in the Department of Electrical and Electronics Engineering Koneru Lakshmaiah Education Foundation (KL Deemed to be University) College of Engineering, has about 16 years of teaching experience. He received his B.Tech. degree in electrical and electronics engineering with distinction from JNTU Hyderabad and M.E. degree in power electronics and drives with distinction from Anna University, Chennai. He received Ph.D. degree in electrical and electronics engineering from KL Deemed to be University, Guntur, Andhra Pradesh. He has published more than 70 Scopus, SCI, and ESCI research papers in refereed international journals and 16 research papers in the proceedings of various international conferences and three patents in his credit. He received Best Teacher Award five times, and his research interest includes switched reluctance machines, power electronics, electric vehicles, and control systems. He is an active member of SIEEE, MISTE, and IEI. He can be contacted at email: kiran.malligunta@gmail.com.

D. Ravi Kumar completed his B.Tech. in EEE in 2006 and M.Tech. in power systems from JNTU, Hyderabad in 2008 and Ph.D. in electrical engineering from JNTU Anantapur in 2017. He has 13 Years of teaching experience. He has published 30 research papers in international, national journals, and conferences. He visited Singapore and presented a paper in IEEE International Conference ICBEST-2015 at CREATE, Singapore. Some of his papers are indexed by Scopus and Web of Science. He has executed UGC Minor Research Project on "Development of Optimization Techniques for Protective Devices and Distributed Generators allocation to optimize Reliability and to reduce losses in Electrical Power Distribution systems with a sanctioned amount of Rs. 4.95 Lakhs". He is currently working as an associate professor in the Department of Electrical and Electronics Engineering and JNTUH, AICTE Coordinator of VNR Vignana Jyothi Institute of Engineering and Technology, Hyderabad, India. He can be contacted at email: ravikumar_d@vnrvjiet.in.

Ch. Rami Reddy received B.Tech. degree in electrical and electronics engineering, M.Tech. degree in electrical machines and drives from Jawaharlal Nehru Technological University, Kakinada, Andhra Pradesh, in 2011, 2014 respectively and the Ph.D. degree in electrical and electronics engineering from K. L. University, Andhra Pradesh, India, in February 2022. He did post doctoral fellowship in micro grids from National Institute of Technology, Srinagar and doing another post doctoral fellowship in micro grids from Chonnam National University, South Korea. He is working as an associate professor in electrical and electronics engineering with Joginpally B R Engineering College, Hyderabad, India. His current research interests include integrated renewable energy systems, distributed generation, FACTS devices, power converters and their applications to energy systems. He can be contacted at email: crreddy229@gmail.com.